Structural Engineering and Mechanics, *Vol. 62, No. 2 (2017) 163-170*
DOI: https://doi.org/10.12989/sem.2017.62.2.163

Motion behavior research of liquid micro-particles filtration at various locations in a rotational flow field

Yan Yan, Yuanzai Lin, Jie Cheng and Zhonghua Ni*

Department of Mechanical and Engineering, Southeast University, 79 Su Yuan Avenue, Nan Jing, 211189, China

(Received September 16, 2016, Revised November 24, 2016, Accepted December 28, 2016)

Abstract. This study presents a particle-wall filtration model for predicting the particle motion behavior in a typical rotational flow field-filtration in blower system of cooker hood. Based on computational fluid dynamics model, air flow and particles has been simulated by Lagrangian-particle/ Eulerian-gas approaches and get verified by experiment data from a manufacturer. Airflow volume, particle diameter and local structure, which are related to the particle filtration has been studied. Results indicates that: (1) there exists an optimal airflow volume of 1243 m^3/h related to the most appropriate filtration rate; (2) Diameter of particle is the significant property related to the filtration rate. Big size particles can represent the filtration performance of blower; (3) More than 86% grease particles are caught by impeller blades firstly, and then splashed onto the corresponding location of worm box internal wall. These results would help to study the micro-particle motion behavior and evaluate the filtration rate and structure design of blower.

Keywords: Computational Fluid Dynamics (CFD); two-phase model; particle-wall filtration model; blower

1. Introduction

Blower system in a cooker hood is a typical rotational flow field, which contains a rotating structure in the flow field. It is widely used to filter grease particles and also can be applied to other processes in chemical industry and fluid machinery. For example, a centrifugal blower can be used to collect the fluid from impeller and transfer to the delivery pipe. Parametric influence on the volute shape was studied by Hariharan and Govardhan (2016), Kabalyk *et al*. (2016) to improve the mass transfer efficiency. Filippone and Bojdo (2010) investigated the blower as a high speed gas generator. Fernández-Yáñez *et al*. (2016) studied the wind resistance in a blower as wind replacement. In addition, it has many transformation such as rotating fluidized bed study from Nakamura and Watano (2007), regenerative blower in waste water circulators from Heo *et al*. (2016) and spin haler in a dry powder inhaler for pulmonary drug delivery in the publication of Islam and Cleary (2012).

Through the rotating blades, the flow field can force both continuous phase and particles being transited, mixed, fluidized, etc. Particle motion is high related to the shape of flow channel, properties of particle and characters of internal walls. Therefore, motion behavior research of micro-particles in a rotational flow field is significant for increasing the controlling efficiency of the flow channel and hence become a very popular academic topic.

Qi *et al*. (2012) studied the solid particle suspension in a stirred tank. In his research, both solid particles and liquid were treated as continua and the Eulerian method was applied to build the computational fluid dynamic (CFD) model of solid-liquid two-phase flow. This model divided the flow field into two domains, an annular steady area and a columnar rotating area. Interfaces and multiple reference frame (MRF) were used to transmit and calculate the fluid data. However, the resistance and turbulence between two phases increased with the impeller rotating speed, and it will become more obvious with higher liquid viscosity. To solve this issue, Wadnerkar *et al*. (2012) added a drag model in Nana's model to describe the flow field at higher impeller speeds. He investigated the impact of drag model on turbulent kinetic energy, suspension quality and height of 4 different drag models. Rahimi *et al*. (2010) applied experimental and CFD methods to modify helical ribbon impeller and improved the mixing performance of the blades. By comparing axial flow number and axial circulation time at different impeller clearance, he concluded that impeller clearance was the key fact on the mixing characteristics of solid and liquid. CFD-predicted flow patterns was used to display the volume fractions at various axial distances from the tank bottom, which was in agreement with the experimental observations.

The above models were efficient in computing the distribution of particles by treating particles as continua. However, it still has some difficulty in defining the motion characters of particle. Therefore, Nakamura *et al*. (2013) used a discrete element method (DEM) to describe the fluidization behaviors of particles in a rotating fluidized bed. He analyzed the particle velocity and mixing behavior at different inclination angles of inflow direction. This DEM-CFD coupling model was set to describe every particle's motion, so that it can obtain the accurate particle trajectory but cannot be used to compute a particularly large number of particles. By contrast, Lagrangian method

*Corresponding author, Professor
E-mail: nzh2003@seu.edu.cn

http://www.techno-press.org/?journal=sem&subpage=8 ISSN: 1225-4568 (Print), 1598-6217 (Online)

classified particles by their size, mass, property, etc. Only several particle groups were calculated to get the motion trajectory, which was computationally more efficient than DEM method and more accurate than Eulerian method. Thus this method was increasingly applied to describe particle filtration and deposition. Milenkovic *et al*. (2013) used Lagrangian-particle/ Eulerian-gas approach to study the steady-state flow and particle deposition in a commercial dry powder inhaler device. In his research, Particle collisions with the walls are taken to result in deposition when the normal collision velocity is less than a critical capture velocity. Particle deposition is highly related to particle size and flow rate. They mostly occurred in the circulation chamber and the helical region of the mouthpiece.

By analyzing the current results about motion research of micro-particles in a rotational flow field from Zhang and Chen (2009), we can see that most of them are describing solid particles in a solid-liquid two-phase flow model. But grease filtration in a cooker hood is a process of liquid particles interaction with internal channel surfaces, which is few to be reported.

In this work, the steady air flow and liquid particle filtration in a blower system are determined by CFD-based computational model, which is solved by ANSYS-CFX 14.5. Results with different airflow volume, particle diameter and deposition location are compared to understand the influence on the grease filtration performance of a typical blower system. The simulation results are compared to the experimental data to verify the CFD model and eventually support the improvement of cooker hood structure.

2. Hydrodynamic model

2.1 Air fluid model

The CFD approach consists of solving continuity and momentum equations in each cell of a discretized computational domain that represents the air passage in blower system. As known from the engineering data, the biggest diameter of grease particles is 2.643×10^{-6} m and the largest particle volume is 9.66×10^{-18} m^3. Even considering the injected particle number about 4.16×10^5, the entire volume of grease is still far form the value 4.14×10^{-2} m^3 of air volume in U-shell. With such a small volume fraction of grease particles, one-way coupling model is used to simulate the grease droplet behavior in air flow. It means that the grease particles are driven by air gas but has no effect on air gas flow. Based on the result from Zhou *et al*. (2017), air gas flow is only related to pressure gradient and blower structure. The continuity and momentum equations of air flow have been written in the general format as follows:

Air gas is treated as incompressible fluid and the properties is set at the reference temperature of 25℃. Therefore the term from density is omitted and the continuity equation is

$$\nabla\cdot\boldsymbol{u}=0 \tag{1}$$

where $\boldsymbol{u}$ is the air velocity vector.

Momentum transfer equation

$$\frac{\partial\boldsymbol{u}}{\partial t}+\nabla\cdot(\boldsymbol{u}\times\boldsymbol{u})=\frac{1}{\rho}(-\nabla\cdot P+\nabla\cdot\tau)+f \tag{2}$$

$$\tau=\mu[\nabla\times\boldsymbol{u}+(\nabla\times\boldsymbol{u})^T] \tag{3}$$

where ρ is the air density, p is the static pressure, τ is the stress tensor, μ is the liquid viscosity and f represents the external accelerations.

Eqs. (1)-(3) can be computed in a solver by either laminar or turbulent flow model with either dynamic or steady-state flow model. For a blower system of cooker hood, airflow volume per minute is related to impeller speed, which is predetermined. So airflow volume changes little after impeller reaching its pre-set value. Consequently, the dynamic airflow developed in the blower system can be approximated by steady-state airflow.

In general, several two-equation Reynolds-averaged Navier–Stokes, RANS models for turbulent flow can be employed based on the Reynolds number and flow pattern. In this paper, CFD simulation are performed to display complicated flow near surface, so standard k-ε turbulent in the model of Qi *et al*. (2012) is selected for its efficient adaption near the boundary layer and low requirement of calculation resource and boundary mesh quality.

2.2 Particle motion model

Grease particle trajectory and filtration behavior are revealed by Lagrangian method in the publication of Ke *et al*. (2011), which differs from the Eulerian method of continuous phase. Lagrangian method is to solve the force balance equation for several particle groups. In this paper, impact from flow field is much larger than gravitational force, which has been neglected. The force balance of a particle is defined as

$$\frac{d\boldsymbol{u}_p}{dt}=F_D(u_a-u_p) \tag{4}$$

where u_a and u_p are the velocity of air and particle, respectively. F_D is drag force per unit mass and given by

$$F_D=\frac{18\mu}{\rho_p d_p^2}\frac{C_D Re_p}{24} \tag{5}$$

where μ is the viscosity of the air fluid, ρ_p and d_p are the density and diameter of grease particle, Re_p is the Reynolds number related to particle in the model of Morsi and Alexande.Aj (1972). The grease is also an incompressible material in the simulation, whose density is fixed at 923.6 kg/m^3.

2.3 Liquid particle filtration model

In the impact theory and micro-particles impact model from Brach and Dunn (1992) and Brach and Dunn (1998), rigid body will rebound from the wall with some energy loss. Only if the incidence velocity is under a value, the particle would stick on the surface. However, considering

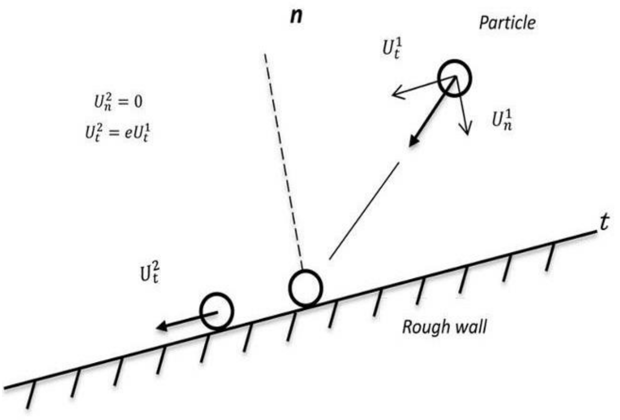

Fig. 1 Particle-wall interaction model

the big adhesion ability of cooking grease, this paper proposes a slipping model as particle-wall filtration model. When a grease particle impacts on a surface at any velocity, it would slip for a certain distance and remains on the surface, as demonstrated in Fig. 1. When the slipping velocity of particle goes down to zero, the grease droplets will be treated as part of the wall and share the same behavior with wall. This process is consistent with the real condition in a cooker hood, where the available ways to detach grease from solid structure are just chemical removing or physical wiping. By neglecting particle angular velocity, the grease particle-wall filtration model is expressed as

$$U_n^2 = 0; \quad U_t^2 = eU_t^1 \tag{6}$$

where e stands for the parallel coefficient of interaction between particle and wall, which is set to 0.1 in this model.

2.4 Simulation set-up

Blower system contains 3 domains: U-shell, worm box and impeller, as shown in Fig. 2(a). Only impeller domain is rotating and the others are stable. The size parameters of Fig. 2(b) are defined as: L1=0.174, L2=0.355, L3=0.389, D1=0.240, D2=0.175, D3=0.124 m. The stretch length of worm box is 0.18 m and U-shell is 0.3 m. Cooking streams rise from the bottom of U-shell before getting accelerated by impeller from both 2 sides, and then the high speed flow is gathered by worm box and discharged from outlet.

For computation, grids of 3 domains are calculated independently and then assembled according to Liu and Yang (2014), as shown in Fig. 3. The amount of tetrahedrons element is about 3 million. To verify the quality of the grid, we check two parameters: maximum skewness is 0.934<0.95 and minimum element quality is 0.105>0.1. Compared with the simulation model from Lanzafame *et al*. (2013), Murthy *et al*. (2007), the mesh of this system is good enough to do study.

Interfaces are used to transmit mass and momentum information between each domain. Alternate rotation and Frozen Rotor frame mixing models are set to the rotating domain. Internal surfaces are treated as no-slip, roughness wall. Opening relative pressure is defined on both inlet and outlet of the system. The convergence criterion is set at 10^{-4} for all equations. Particle Transport Fluid and Diameter Distribution are applied to describe grease particles assuming that all particles are injected from the inlet wall beneath U-shell uniformly. The diameter distribution of the grease particle is taken from the kitchen room experiment, as shown in Fig. 4. This data comes from the Pre-development of Cooker Hoods in Bosch and Siemens Home Appliance Group (Nanjing, China).

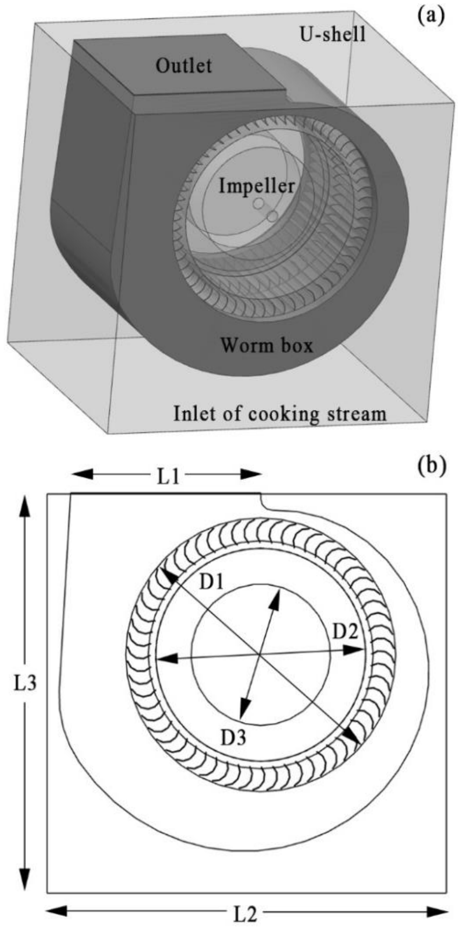

Fig. 2 Structure of blower system in cooker hood

In Lagrangian method, all particles in an assuming group share the same motion behavior, so the number of real particles in a particle group influents the accuracy of the result and is determined by the mass fraction and number fraction of a specific diameter

$$N = \frac{6 * m * m_{fn}}{10000 * N_{fn} * \rho_p * \pi * D_n^3} \tag{7}$$

where N is the number of real particles, m is the mass of the group, ρ_p is grease density, D_n is the specific particle diameter and related to its number fraction N_{fn} and mass fraction m_{fn}.

In this paper, location number of particle injection is 10,000, which means 10,000 particle groups in the simulation and the number of particle in a group calculated from Eq. (7) is 41.6, which is acceptable in this grease particle filtration simulation.

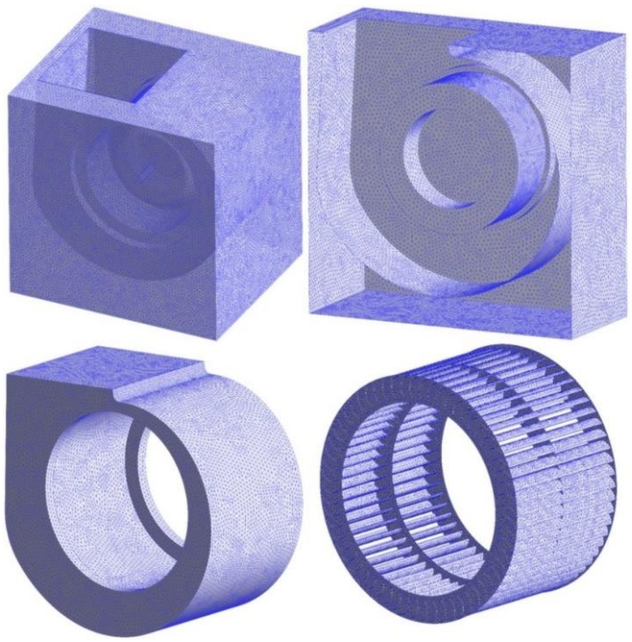

Fig. 3 Grid of 3 divided domains. After calculated separately, all domains are connected by interfaces

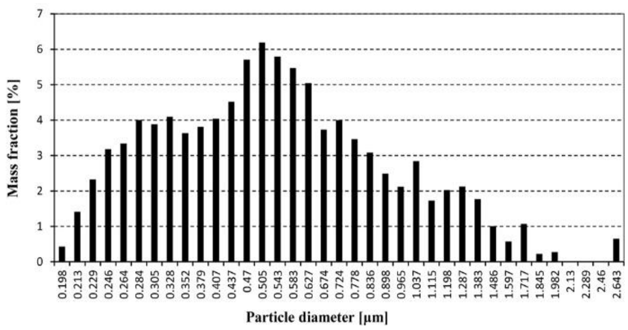

Fig. 4 Grease particle distribution used in the simulation

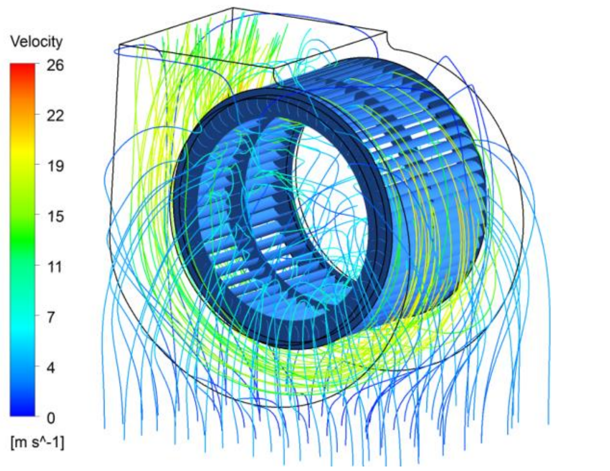

Fig. 5 Streamlines of air fluid in blower system (Rotation speed=920 rev/min)

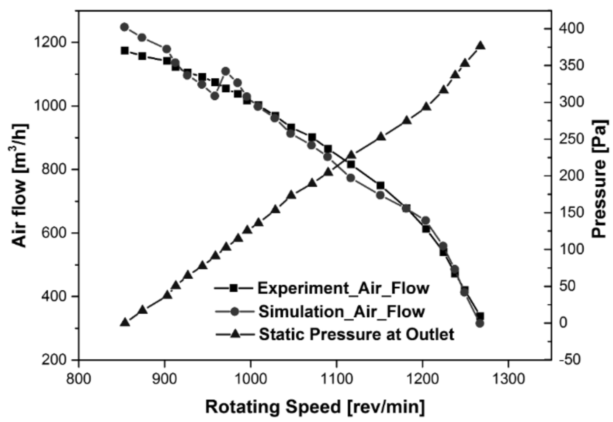

Fig. 6 Compare the airflow volume between simulation model and experiment

3. Result

3.1 Verification of model

To check the logical reliability of the CFD model, streamlines of air flow are compared with the real air fluid process. Streamlines in Fig. 5 display the entire process of air flow. This air flow process starts from the open bottom of U-shell, which is named as inlet of blower system. And then flows through the U-shell, impeller blades and worm box. At last, it ends on the top outlet of worm box. Near the inlet, air is sucked into blower by the negative pressure and then lifted to the height of impeller entrance and accelerated by the centrifugal force of rotating blades. At last, high velocity air is gathered in worm box and then escape form the outlet at about 15 m/s. This process is corresponding to the real condition of cooker hood in experiment.

To verify the accuracy of the CFD model, it is the airflow volume per minute at outlet to be compared between simulation result and the experiment data from the Pre-development of Cooker Hoods in Bosch and Siemens Home Appliance Group (Nanjing, China).

There are 23 different conditions are considered in Fig. 6. In the experiment drag pressure is the drive parameter of impeller speed and airflow volume at outlet, which means impeller speed need to adapt to the condition of drag pressure based on its motor feedback system. However, in CFD model, impeller speed and drag pressure are predefined and just airflow volume at outlet is calculated and could be compared with the experiment data. In Fig. 6, the simulation airflow volume-line with circles is closed to the experiment one-line with squares. The biggest difference is 6.7%, which is acceptable to reflect the air flow field and taken as a base to do the particle-air two-phase analysis.

3.2 Particle filtration-effect of airflow volume

As the particle motion and filtration model have been defined in Section 2.2 and 2.3, it's available to simulate the movement of all particles and then get the travelling process in a blower system. From the computational result, we could study the difference of filtration performance in every local structures and various particle sizes, but not only the final situation of grease film in experiments. And then it will help to improve the design of experiment, such as how to decide the testing droplet size, or which condition should

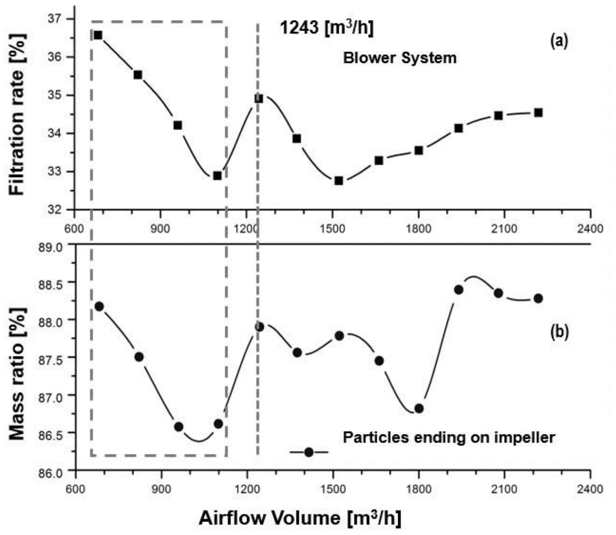

Fig. 7 Compare the filtration rate of blower system and the mass ratio of local structure

be more considered. Consequently, the numerical simulation can become an efficient method to analyze and optimize the blower system. In the following parts, three factors of airflow volume, particle diameter and local structure have been studied to understand the influence of grease filtration in a blower system of cooker hood.

Airflow volume per minute at outlet is widely used to identify the working condition of cooker hood both in Research and Development Center of factories and Sales department by Rim *et al*. (2012), Zhao and Chen (2006). So in this work, airflow volume has been analyzed firstly. Filtration performance of blower system is defined as the ratio of mass of filtered particles and inflow particles, following the model from Li and Delsante (1996)

$$Filtration\ rate = \frac{Particles\ ending\ on\ wall}{Particles\ input\ into\ blower} \quad (8)$$

Local mass ratio is the ratio between local filtration and system filtration, defined as

$$Mass\ ratio = \frac{Particles\ captured\ by\ local\ structure}{particles\ captured\ by\ blower\ system} \quad (9)$$

In hood blower, both grease particles and air are sucked from the bottom of blower and accelerated by impeller. This part compared the overall filtration rate and the local filtration rate of impeller under 12 different airflow volume conditions, as shown in Fig. 7. Horizontal coordinates stands for airflow volume. There are above 86% filtered particles being caught by impeller, which means impeller blades structure dominates the filtration performance.

When the airflow volume is smaller than 1099 m^3/h, as shown in the dotted box of Fig. 7, both filtration rate and impeller capture ratio decrease with the airflow growing. However, when the airflow volume is bigger than 1522 m^3/h, the filtration rate increases with the airflow and tends to be stable at 34.5%. However, there exists a local maximum of filtration rate between 1099 and 1522 m^3/h, which is located at 1243 m^3/h. Even the filtration rate is higher in low airflow volume, the airflow volume could not afford the requirement from kitchen room. However, increasing the airflow to a very large value can't help to improve the filtration performance of cooker hood. More cooking fumes sucked means more grease particles are released to the outside, which is harmful to the environment. So this local maximum case becomes a optimal condition in the industry and can be treated as the best working point of this structure of blower system. To reveal the physical insights on this optimal condition, more studies on particle filtration is proceeded below.

Table 1 Filtration condition on different local structures

Air volume (m^3/h)	Total filtration 10^{-11}(kg)	Impeller 10^{-11} (kg)	Shell 10^{-11} (kg)	Worm box 10^{-11} (kg)
1099	3.67	3.18	0.367	0.125
1243	3.90	3.42	0.365	0.107
1522	3.66	3.21	0.365	0.081

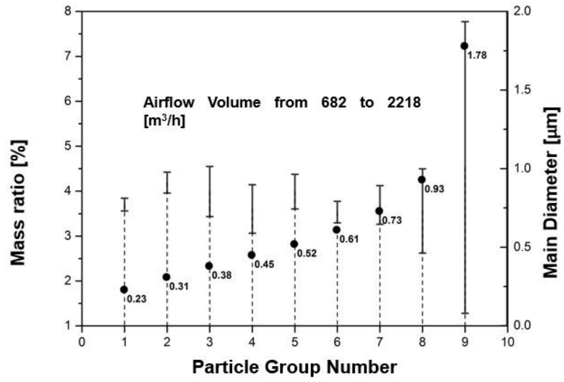

Fig. 8 Filtration rate of particle groups over 12 cases

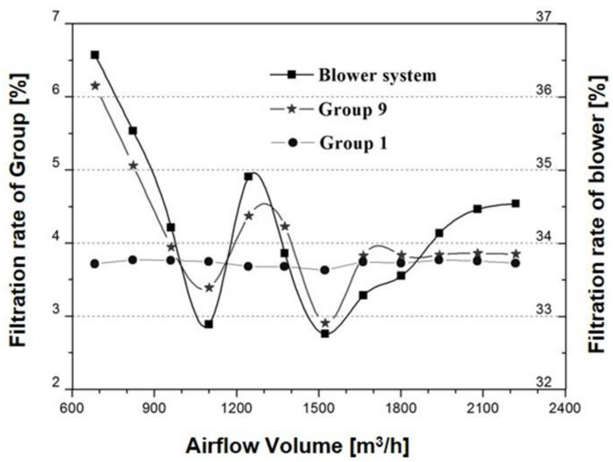

Fig. 9 Compare the filtration rate of blower system and particle group 1 and 9

3.3 Particle filtration-effect of particle diameter

Depending on particle diameter, all injected particles are divided into 9 groups. Mass fraction of each group is close and the main diameter get bigger from Group 1 to Group 9.

Fig. 8 shows the filtration rate range of each group over 12 cases. The influence of airflow volume is very small on Group 1-smaller size particles, but extremely large on Group 9-bigger size particles. To understand this size effect of particles, filtration rate of Group 1 and 9 are displayed in Fig. 9. Compared with the filtration rate of blower, Group 9's filtration (main diameter of 1.78×10^{-6} m) shares the same tendency with blower's, which also has an local maximum filtration rate at 1243 m^3/h. Therefore, we could know that better filtration performance on big size particles is one of the reasons causing local maximum rate at 1243 m^3/h. Another reason comes from the local structure performance. By comparing the filtration conditions near 1243 m^3/h in Table 1, we can find that even it has a less or close amount of grease at shell and worm box, the local maximum case has much higher filtration performance at impeller, which results in a bigger overall filtration.

However, the filtration rate of Group 1 stays stable at 3.7%. It means that in the future study, small size particles are not suggested to be the testing particles, which is inefficient to describe the filtration performance of blower system.

3.4 Particle filtration-effect of location

As discussed in chapter 3.2, most particles are caught by impeller blades. So in the part, accumulation location of particles on impeller blades is discussed. The rotating speed of impeller is 900 rev/min and the related airflow volume is 1243 m^3/h.

Fig. 10 gives the track lines of particles caught by impeller structure. The displayed lines are just the clipped lines located in impeller and worm box domains, without shell domain. So that it would be easier to find the end of these tracks, which stands for the accumulation area of grease. Blue area stands for particles with near-zero velocity and can be considered as the accumulation area of grease droplets on impeller walls.

Fig. 10(a) is a general overview of particle tracks and get amplified in Fig. 10(b). As most air gas should go through the impeller before leave the blower, it provides a big chance to rotating blades capturing the grease particles in the passing air flow. Direction of impeller rotation speed is clockwise, so that most particles are caught by the concave surfaces of blades. In addition, there exist some particles and air gas being redirected by the worm box inner surface and flowing back to impeller near the outlet, as shown in the left bottom of Fig. 10(c). Therefore, the material and roughness of concave surfaces have a big influence on the slipping distance of particles, as well the axial distribution on the blades.

Fig. 10(d) shows the axial distribution of particles, viewing from the right side of Fig. 10(a). After undertaking the centrifugal force for a period of time, these grease particles will depart from blades and splashed onto the corresponding location of worm box. That is to say, the accumulation position on worm box is close to the one of impeller blades. Details of this relationship are shown in Fig. 11. Dotted lines in the middle stand for the symmetry line of worm box. The initial surface of the worm box is gray and the color of grease is yellow. Area-A shows that accumulation range on the backside is larger than the front side. This is confirmed in the simulation result in the left picture. Tracks on the backside have a larger range than the front side. Area-B shows that the distribution is equally matched, front side is little bigger than far side. Picture on the right is fit to this phenomenon, in which lines on the two sides are close to each other; only the top of front side is larger than backside.

In the industry, grease grooves and leaking holes are located at the middle and bottom of internal wall of worm

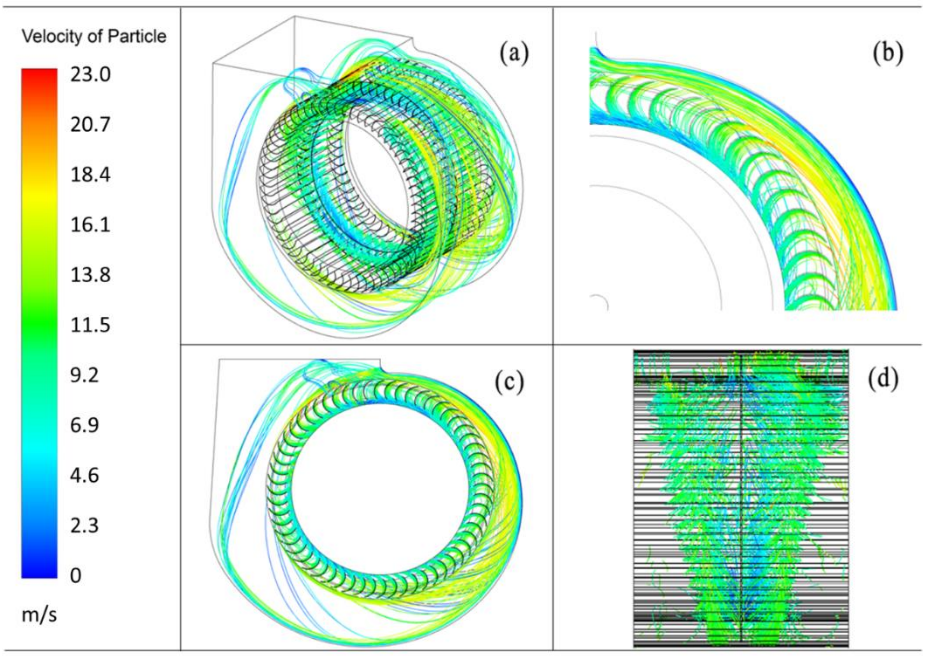

Fig. 10 Particle tracks of the grease caught by impeller surfaces

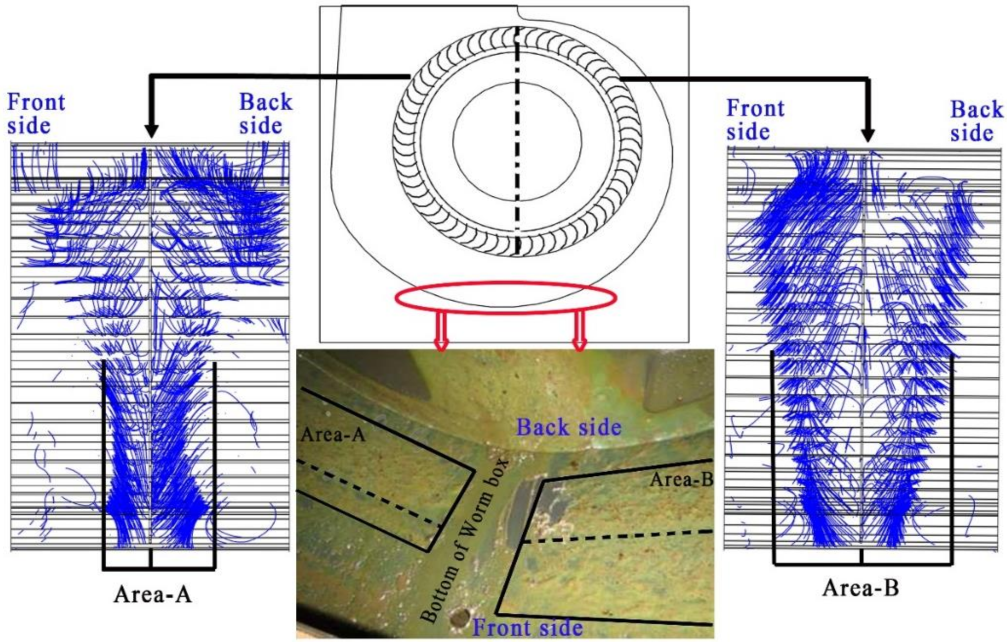

Fig. 11 Comparison between simulation and experiment about the grease accumulation

box. So that, it is the best to catch the grease particles in this area and reduce the residual grease on the surface. Overall, location study can help to evaluate the improvement of blades shape and worm box structure.

4. Conclusions

Filtration rate and accumulation location of cooking grease in blower system are typical motion behaviors of liquid micro-particles in a rotational flow field and studied by simulation model and experiment, leading to the following results:

- To a specific structure blower system, there exists a optimal airflow volume related to the most appropriate filtration rate in the kitchen room, which is 1243 m^3/h in this paper.
- Diameter of particle is the significant property related to the filtration rate. Big particle's has larger force of inertia and its filtration performance can represent the performance of blower. Diameter of $1.78*10^{-6}$ m can be used to evaluated the filtration performance of this blower.
- Over 86% grease particles are caught by impeller blades firstly, and then splashed onto the corresponding location of worm box internal wall. This distribution can be reflected by both simulation and experiment in lab, which has similar results and provides a tool to evaluate the design of impeller, worm box and even the whole blower.

Acknowledgments

The research was supported by the Major Program of the National Natural Science Foundation of China (91023024), the Jiangsu Province for the transformation of scientific and technological achievements (BA2013092,), the Fundamental Research Funds for the Central Universities and scientific research innovation project for graduate students in Jiangsu province (KYLX15_0060), and Jiangsu province research prospective study (BY2014127-06).

Reference

Brach, R.M. and Dunn, P.F. (1992), "A Mathematical model of the impact and adhesion of microsphers", *Aerosol. Sci. Technol.*, **16**, 51-64.

Brach, R.M. and Dunn, P.F. (1998), "Models of rebound and capture for oblique microparticle impacts", *Aerosol. Sci. Technol.*, **29**, 379-388.

Fernández-Yáñez, P., Armas, O. and Martínez-Martínez, S. (2016), "Impact of relative position vehicle-wind blower in a roller test bench under climatic chamber", *Appl. Therm. Eng.*, **106**, 266-274.

Filippone, A. and Bojdo, N. (2010), "Turboshaft engine air particle separation", *Prog. Aerospace Sci.*, **46**, 224-245.

Hariharan, C. and Govardhan, M. (2016), "Improving performance of an industrial centrifugal blower with parallel wall volutes", *Appl. Therm. Eng.*, **109**, 53-64.

Heo, M.W., Seo, T.W., Shim, H.S. and Kim, K.Y. (2016), "Optimization of a regenerative blower to enhance aerodynamic and aeroacoustic performance", *J. Mech. Sci. Technol.*, **30**, 1197-1208.

Islam, N. and Cleary, M.J. (2012), "Developing an efficient and reliable dry powder inhaler for pulmonary drug delivery-A review for multidisciplinary researchers", *Med. Eng. Phys.*, **34**, 409-427.

Kabalyk, K., Kryłłowicz, W., Liśkiewicz, G., Horodko, L. and Magiera, R. (2016), "Experimental investigation of the influence of the inlet duct configuration on the unstable operation of a single-stage centrifugal blower", *Proc. Inst. Mech. Eng., Part A: J. Pow. Energy*, **230**, 260-271.

Ke, S., Lin, L. and Hai, J. (2011), "Modelling of particle deposition and rebound behaviour on ventilation ducting wall using an improved wall model", *Indoor Built Environ.*, **20**, 300-312.

Lanzafame, R., Mauro, S. and Messina, M. (2013), "Wind turbine CFD modeling using a correlation-based transitional model", *Renew Energy*, **52**, 31-39.

Li, Y.G. and Delsante, A. (1996), "Derivation of capture efficiency of kitchen range hoods in a confined space", *Build. Environ.*, **31**, 461-468.

Liu, T. and Yang, J. (2014), "Three-eimensional computations of water-air flow in a bottom spillway during gate opening", *Eng. Appl. Comput. Fluid.*, **8**, 104-115.

Milenkovic, J., Alexopoulos, A.H. and Kiparissides, C. (2013), "Flow and particle deposition in the Turbuhaler: A CFD simulation", *Int. J. Pharmaceut.*, **448**, 205-213.

Morsi, S.A. and Alexande, A. (1972), "Investigation of particle trajectories in 2-phase flow systems", *J. Fluid. Mech.*, **55**, 193-208.

Murthy, B.N., Deshmukh, N.A., Patwardhan, A.W. and Joshi, J.B. (2007), "Hollow self-inducing impellers: Flow visualization and CFD simulation", *Chem. Eng. Sci.*, **62**, 3839-3848.

Nakamura, H., Kondo, T. and Watano, S. (2013), "Improvement of particle mixing and fluidization quality in rotating fluidized bed by inclined injection of fluidizing air", *Chem. Eng. Sci.*, **91**, 70-78.

Nakamura, H. and Watano, S. (2007), "Numerical modeling of particle fluidization behavior in a rotating fluidized bed", *Powd. Technol.*, **171**, 106-117.

Qi, N., Zhang, H., Zhang, K., Xu, G. and Yang, Y. (2012), "CFD simulation of particle suspension in a stirred tank", *Particuology*, **11**(3), 317-326.

Rahimi, M., Kakekhani, A. and Alsairafi, A.A. (2010), "Experimental and computational fluid dynamic (CFD) studies on mixing characteristics of a modified helical ribbon impeller", *Korean J. Chem. Eng.*, **27**, 1150-1158.

Rim, D., Wallace, L., Nabinger, S. and Persily, A. (2012), "Reduction of exposure to ultrafine particles by kitchen exhaust hoods: the effects of exhaust flow rates, particle size, and burner position", *Sci. tTotal Environ.*, **432**, 350-356.

Zhang, Z. and Chen, Q. (2009), "Prediction of particle deposition onto indoor surfaces by CFD with a modified Lagrangian method", *Atmos. Environ.*, **43**, 319-328.

Zhao, B. and Chen, J. (2006), "Numerical analysis of particle deposition in ventilation duct", *Build. Environ.*, **41**, 710-718.

Zhou, T., Ye, T., Zhu, M., Zhao, M. and Chen, J. (2017), "Effect of droplet diameter and global equivalence ratio on n-heptane spray auto-ignition", *Fuel*, **187**, 137-145.

CC